2º CONGRESSO BRASILEIRO DE P&D EM PETRÓLEO & GÁS

SIMULATION OF TURBULENT FLOW IN A RIETEMA HYDROCYCLONE

Francisco José de Souza[1], Aristeu da Silveira Neto[2]

[1] Universidade Federal de Uberlândia, Av João Naves de Ávila, 2160, Uberlândia, fjsouza@mecanica.ufu.br
[2] Universidade Federal de Uberlândia, Av João Naves de Ávila, 2160, Uberlândia, aristeus@mecanica.ufu.br

Abstract – Large-eddy simulation (LES) has been used to predict the dynamic behavior of a water-fed hydrocyclone operating without an air core. The three-dimensional, time-dependent Navier-Stokes equations have been solved by a fractional step method on a staggered grid. The Smagorinsky subgrid-scale model was employed to account for turbulence effects. Numerical results actually capture the main features as well as instabilities of the flow and agree well with experiments.

Keywords: Large-eddy simulation, hydrocyclone, instabilities

1. Introduction

Hydrocyclones are solid-liquid separation devices widely used in chemical, mineral, textile and powder-processing industries. In spite of their simplicity in terms of construction, the internal fluid dynamics is rather complex, involving phenomena such as high preservation of vorticity, vortex breakdown and reverse flow. In designing a hydrocyclone for a particular application, design equations are usually employed, which are based on correlations obtained experimentally. Characteristics such as the classification curve and pressure drop versus volumetric flow rate can be obtained. However, these correlations tend to be available for a limited number of experimental conditions. Alternatively, computational fluid dynamics techniques can be utilized in the study of the dynamic behavior of this device. Besides providing a physical insight into the causes of the phenomena observed, this approach may allow the reliable design of hydrocyclones.

The main difficulty in simulating the dynamic behavior in a hydrocyclone without an air core is that the flow is known to be anisotropic, and therefore the conventional k-ε and Prandtl mixing length models fail to predict the flow patterns. Indeed, several authors have shown the inaccuracy of these models in their standard form when employed to simulate the flow inside hydrocyclones (Malhotra et all, 1994) and air cyclones (Meier et all, 1999). Considerable effort has been expended in the adaptation of these models to account for anisotropic effects in cyclones and hydrocyclones and successful results have been reported (Malhotra et all, 1994; Meier et all, 1999 and Hsieh et all, 1991). However, the modifications in the turbulence models either increased their complexity (Dyakowsky et all, 1991; Malhotra et all, 1994 and Meier et all, 1994) or required new constants to be fit or experimental information.

The present contribution aims to use LES to simulate the flow in a hydrocyclone to account for the turbulence effects. This approach requires that the large, anisotropic eddies be resolved directly whereas the smallest, subgrid-scale eddies be modeled. As the small scales tend to be more nearly isotropic, this turbulence modeling needs not be revised like the classical models and appears to be suitable for simulating flows in hydrocyclones. The Smagorinsky model is the simplest subgrid-scale model and is experimented with in this work. A chief advantage of this model lies in its simplicity and dependence on a single constant only, whose value ranges from 0.1 to 0.24. Furthermore, LES allows the instantaneous behavior of the flow to be captured, thus providing precious information regarding the physics of the flow and consequently its intrinsic mechanisms.

In order to compute the large scales of flow, the three-dimensional time-dependent Navier-Stokes equations are solved with a finite-difference scheme which is second-order accurate in time and space. A fractional step method is employed to couple velocity and pressure and assure that the flow field is divergence-free at the end of each time step. The central difference scheme is chosen for the convective terms because of its energy-conserving properties. Grids as fine as 100000 nodes are employed to simulate four Reynolds numbers ranging from 14300 to 26600.

Time-averaged numerical profiles and experimental data display fairly good agreement. The instantaneous flow is seen to be asymmetric about the vertical axis. A low-frequency instability of the core of the main vortex about the vertical axis can be observed in snapshots of the vector plots. This motion is known as precessing vortex core (PVC) (Griffiths et all, 1998), which has a considerable effect on the velocity fluctuations in rotating flows.

2. Mathematical Model

Since Large Eddy Simulations are inherently three-dimensional and time-dependent, the mathematical model comprises the continuity equation and the full Navier-Stokes equations for incompressible flow in cylindrical coordinates. These equations must be filtered in order to separate the large scales and the subgrid scales (Lesieur, 1990).

This filtering process gives rise to additional stress tensors, which are modeled using the classical Boussinesq hypothesis. As a consequence, the viscosity in the filtered equations is the effective viscosity(ν_{eff}), given by the sum of the molecular viscosity (ν) and the turbulent viscosity (ν_t):

$$\nu_{eff} = \nu + \nu_t \,. \tag{1}$$

The turbulent viscosity in this work is computed with the Smagorinsky (1963) subgrid-scale model:

$$\nu_t = \left(C_s d\Delta\right)^2 \left(S_{ij}S_{ij}\right)^{1/2}, \tag{2}$$

$$\Delta = \left(r\Delta\theta\Delta r\Delta z\right)^{1/3}, \tag{3}$$

where C_s is a constant between 0.1 and 0.24 related to the energy transfer from the large scales to the small ones. This constant depends on the flow type and must be tuned with experimental information. In this work, the experimental results have led the best value for C_s to be 0.15. Δ is the grid filter size, Δr, Δz and $\Delta\theta$ are the grid spacings in the r, z and θ directions, respectively and S_{ij} is the strain rate, which is calculated with the resolved values of the filtered velocities. Because the turbulent viscosity must be zero on the wall, C_s is multiplied by a damping factor d which reads (Jacobsen, 1997):

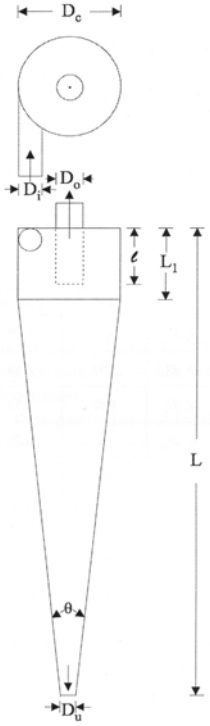

Figure 1. Schematics of a conventional hydrocyclone (Massarani, 1997).

Table 1. Dimensions of the hydrocyclone investigated (m).

D_c	0.0762
D_o	0.0265
D_i	0.0218
D_u	0.0124
L	0.381
ℓ	0.0305
L_1	0.0381

$$d = 1 - \exp(-r^+ / 30)^2 , \tag{4}$$

$$r^+ = \frac{(r - r_w)}{\nu}\left(\frac{\tau_w}{\rho}\right)^{1/2} , \tag{5}$$

where τ_w represents the shear stress on the wall, $r\text{-}r_w$ is the distance from the node to the nearest wall and ρ is the fluid density.

No slip conditions have been used for the three velocity components on all the walls. Therefore, no wall functions have been used. In the experiments carried out by Dabir (1983), the flow ratio between the upper exit and the inlet was kept at 80 %. In order to keep the same flow ratio in the simulations, flat velocity profiles have been specified at the upper and lower exits. The velocities assigned were calculated from the respective flow rates at the outlets. At the inlet, the intersection between the inlet pipe and the cyclone was modeled as the flow inlet. The respective radial and tangential velocity components could then be determined based on the flow rate and the intersecting points.

The Reynolds number has been defined as:

$$Re = (4Q)/\pi D_i \nu , \tag{6}$$

where Q is the inlet volumetric flow rate and D_i is the inlet diameter of the cyclone.

3. Numerical Method

The set of governing equations are solved by a fractional step method (Armfield et all, 1999) on a nonuniform staggered grid. At each time step, the following steps are accomplished:

Predictor step:

$$\frac{u_i^{*} - u_i^{n}}{\Delta t} = \frac{3}{2}\left[-\frac{\partial}{\partial x_j}\left(u_j u_i\right) + \frac{\partial}{\partial x_j}\left(\nu_{eff}\frac{\partial u_i}{\partial x_j} + \nu_{eff}\frac{\partial u_j}{\partial x_i}\right)\right]^{n} - \frac{1}{2}\left[-\frac{\partial}{\partial x_j}\left(u_j u_i\right) + \frac{\partial}{\partial x_j}\left(\nu_{eff}\frac{\partial u_i}{\partial x_j} + \nu_{eff}\frac{\partial u_j}{\partial x_i}\right)\right]^{n-1} - \frac{\partial p^{n}}{\partial x_i} \tag{7}$$

Pressure calculation:

$$\frac{\partial^2 p'}{\partial x_i \partial x_i} = \frac{1}{\Delta t}\frac{\partial u_i^{*}}{\partial x_i}, \tag{8}$$

$$p^{n+1} = p^{n} + p'. \tag{9}$$

Corrector step:

$$\frac{u_i^{n+1} - u_i^{*}}{\Delta t} = -\frac{\partial p'}{\partial x_i}. \tag{10}$$

The central difference scheme was used to discretize the convective and the diffusive terms of the velocity components. The equations were advanced explicitly in time with the 2nd order Adams-Bashforth scheme. The pressure correction equation was solved by the modified strongly implicit procedure MSI implemented by Norris (1996).

4. Results

Figure 2a depicts the time-averaged velocity vectors throughout the hydrocyclone (Re=14300) along the center axial-radial plane which bisects vertically across the inlet duct. The flow reversal is clearly seen along the entire conical section, as theoretically predicted (Svarovsky, 1984), as well as the presence of both outer and inner vortices. The mean flow is seen to be asymmetric about the vertical axis. Obviously, an axisymmetric model is not capable of capturing this feature. Also, multiple reversals in flow direction do exist in the region between the vortex finder and the wall. The reverse flow continues throughout most of the hydrocyclone length. There is a secondary flow pattern at the top of the cylindrical section. It moves across the top cover to the base of the vortex finder and along its outer wall until it merges with the rest of the fluid in the upper exit. This is referred to as short-circuit, which has a negative effect on the collection efficiency of coarse and fine particles. Figure 2b presents the time-averaged velocity vectors along a plane which is orthogonal to the plane shown in Fig. 2a for Re=14300. Recirculation eddies can be seen, some of which rotate in the opposite direction of those in Fig. 2a. These recirculation eddies prevent any radial flow through a cylindrical surface within the flow so that it causes the resistance to radial flow to become higher than to axial flow. This effect tends to make the motion highly anisotropic. From these figures the helical trend of the flow becomes clearly visible.

Figure 3 displays the contours of the time-averaged tangential velocity from a top view. A flow separation zone is visible at the outer wall of the exit pipe. Actually, it has been observed in industrial cyclones that solid particles tend to accumulate in this region, as a natural consequence of flow reversal.

Though not shown here, snapshots of the instantaneous flow reveal the unsteadiness of the flow and it is possible to recognize some turbulent structures in the conical section which resemble wavy Taylor-Couette instabilities. Also, as the fluid flows towards the underflow exit, its spiral trajectory becomes more evident. Interestingly, it is well known from experiments that in this region the axisymmetric hypothesis fails. The core of the inner vortex is seen to fluctuate around the vertical axis. This effect was called vortex-core precession (Griffiths et all, 1998). This motion appears to be of a quasi-periodic nature. It can be seen from the respective instantaneous pressure contours that the pressure field is particularly highly asymmetric close to the underflow exit, due to the radius reduction and the relatively high flow rate, and in the vortex finder. Besides that, the region of minimum pressure moves about the cyclone center. As the core of the vortex can be associated to the point of least pressure, this is strong evidence that the vortex core seems to avoid the center of the hydrocyclone. It is important to emphasize that these are coherent fluctuations, and can be solved in the present simulation because we are using a subgrid-scale model. Such a turbulence model is supposed to act only on the turbulent fluctuations, whereas in a RANS simulation the turbulence model affects fluctuations at all scales. As a consequence, in a RANS computation normally only very low frequencies can be resolved, since the higher-frequency fluctuations are damped out by the turbulence model.

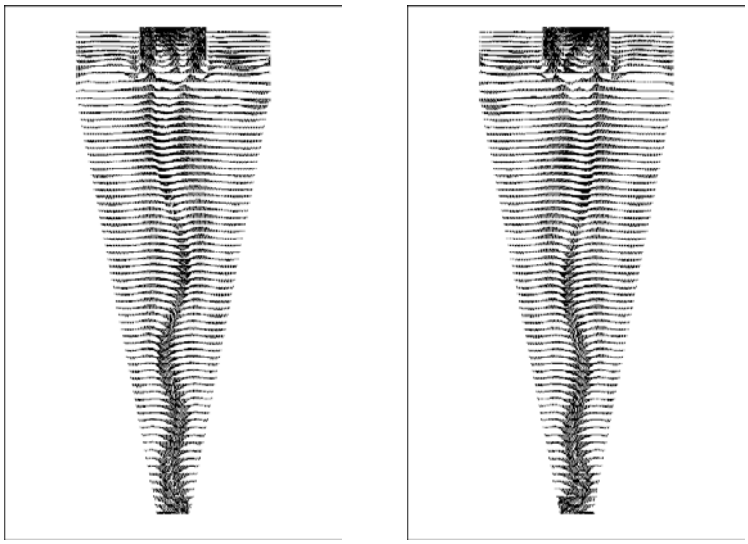

2a 2b

Figures 2(a-b). Time-averaged velocity vectors along two orthogonal r-z plane (Re=14300).

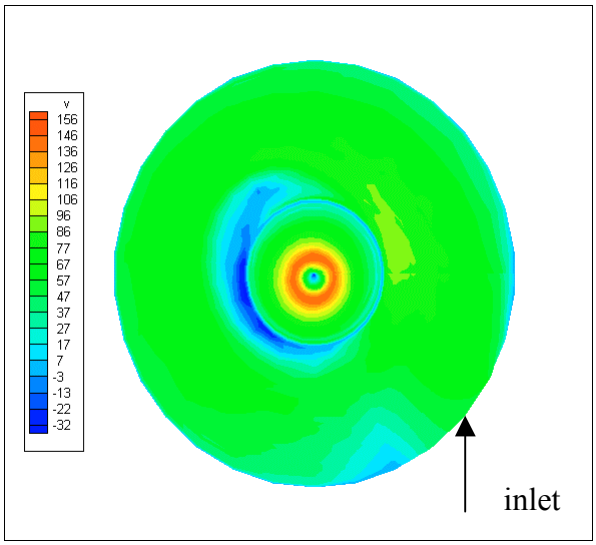

Figure 3. Time-averaged swirl velocity contours (x 10^2 m/s) - top view (Re=14300).

Shown in Figure 4 are the results of simulations for the swirl velocities and experimental data at z=0.20 m at four Reynolds numbers investigated. The mean numerical profiles display good agreement with experimental data, though underpredicting the swirl magnitude near the wall and slightly overpredicting it close to the peak. Such effect is believed to be due to the poor grid resolution near the wall. It is important to highlight that, unlike most RANS simulations, no wall functions have been used. Therefore, it is expected that finer grids and/or adaptive grid refinement will provide better agreement.

All the results presented in this work have utilized C_s=0.15 associated to a grid resolution of nearly 100000 nodes. However, for each Reynolds number, it would be possible to fit values for C_s slightly different and refine the mesh in order to improve the agreement with experiments. This is a consequence of the fact that the Smagorinsky constant actually varies from place to place within the flow (Wilcox, 1994) and hence, the value tuned improves the overall agreement between simulated and experimental results at different turbulence levels.

A strict validation of the predicted results should also take into account axial velocity profiles. Even though such profiles are not available, accurate results for the tangential component suggest that the other components have been well predicted, as verified by Hsieh et all (1991). It is hoped that the present methodology will be used in a near future as a tool for the study, design and optimization of hydrocyclones.

Although the Smagorinsky model still presents the drawback of requiring the tuning of a constant, it provides advantages over turbulence models classically used for hydrocyclone simulation. In LES, the most anisotropic eddies are resolved directly, whereas only the smallest, less anisotropic eddies are modeled. Therefore, it is expected that the subgrid-scale models available, e.g. dynamic, mixed-scales, can be used in their standard form, unlike the k-ε model, which requires further revision and possibly new constants.

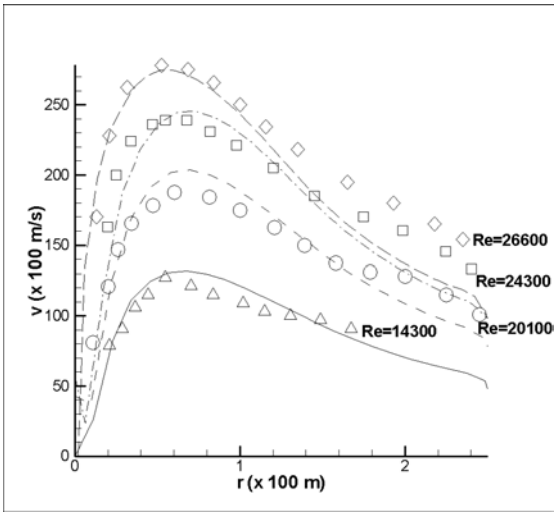

Figure 4. Comparison with experimental data (symbols) by Dabir (1983) at z=0.20 m.

5. Conclusions

The results of LES of the unstable flow in a hydrocyclone are very encouraging and have shown that it represents a promising alternative to classical turbulence modeling. The general trends of the variations have been consistently predicted with the Smagorinsky model in its standard form. The dynamic behavior of the flow has been captured, providing important information on the phenomena that take place within the equipment.

6. Acknowledgement

The authors wish to thank CNPq for the financial support provided for this work.

7. References

ARMFIELD, S. and STREET, R. The fractional step method for the Navier-Stokes equations on staggered grids: the accuracy of three variations. *Journal of Computational Physics*, 153, p. 660-665, 1999.

DABIR, B. Mean velocity measurements in a 3" hydrocyclone using Laser Doppler Anemometry, Ph.D. thesis, Chemical Engineering Department, Michigan State University, East Lansing, MI, 1983.

DUGGINS, R. K. and FRITCH, P.C.W. Turbulence effects in hydrocyclones. In: *3rd International Conference in Hydrocyclones*, Oxford, p. 75-81, 1987.

DYAKOWSKY, T. and WILLIAMS, R. A. Modelling turbulent flow within a small-diameter hydrocyclone. *Chemical Engineering Science*, v. 48, n. 6, p. 1143-1152, 1993.

GRIFFITHS, A. J., YAZDABADI, P. A. and SYRED, N. Alternative eddy shedding set up by the nonaxisymmetric recirculation zone at the exhaust of a cyclone dust separator. *J. Fluids Eng*, 120, 193, 1998.

HSIEH, K. T. and RAJAMANI, R. K. Mathematical model of the hydrocyclone based on the physics of fluid flow. *AIChe Journal*, v. 37, n. 5, p. 735-745, 1991.

JACOBSEN, C. B. Large-eddy simulation of confined swirling flow, Ph.D. thesis, Institute of Energy Technology, Aalborg University, Aalborg, Denmark, 1997.

LESIEUR, M. *Turbulence in Fluids*, Kluwer Academic Publishers, 1990.

MALHOTRA, A., BRANION, R. M. R. and HAUPTMANN, E. G. Modelling the flow inside a hydrocyclone. *The Canadian Journal of Chemical Engineering*, 72, p. 953-960, 1994.

MASSARANI, G. *Fluidodinâmica em Sistemas Particulados*, Editora UFRJ, Rio de Janeiro, 1997.

MEIER, H. F. and MORI, M. Anisotropic behavior of the Reynolds stress in gas and gas-solid flows in cyclones, *Powder Technology*, v. 101, p. 108-119, 1999.

NORRIS, S. E. An Investigation into the Comparative Speeds of Linear Solvers in the Solution of PDE´s, Ph.D. thesis, School of Mechanical Engineering, University of South Wales, Australia, 1996.

SMAGORINSKY, J. General Circulation Experiments with the Primitive Equations, I. The basic experiment. *Monthly Weather Review Rev* 91, p. 99-164, 1963.

STONE, H. L. Iterative Solution of Implicit Approximations of Multidimensional Partial Differential Equations. SIAM *J. Numer. Anal*., v. 5, n. 3, p. 530-558, 1968.

SVAROVSKY, L. *Hydrocyclones*, Holt, Rinehart & Winston Ltd, London, 1984.

WILCOX, D. C. *Turbulence modeling for CFD*, DCW Industries, Inc, 1994.